准单能γ用于核反应

张焕乔 张春雷 白春林
中国原子能科学研究院
高能物理研究所
四川大学

The aim of nuclear astrophysics is to work with astrophysics modellers and observational astronomers to:

Understand the abundance pattern of the elements that we see around us and understand the nuclear reaction processes that have created them and the astrophysical sites where these occur (stars or explosive sites like novae, X-ray bursters, supernovae etc.)

Develop models to describe these sites and test the predictions against measurements of element abundances and energy output (optical or gamma observations or pre-solar grains

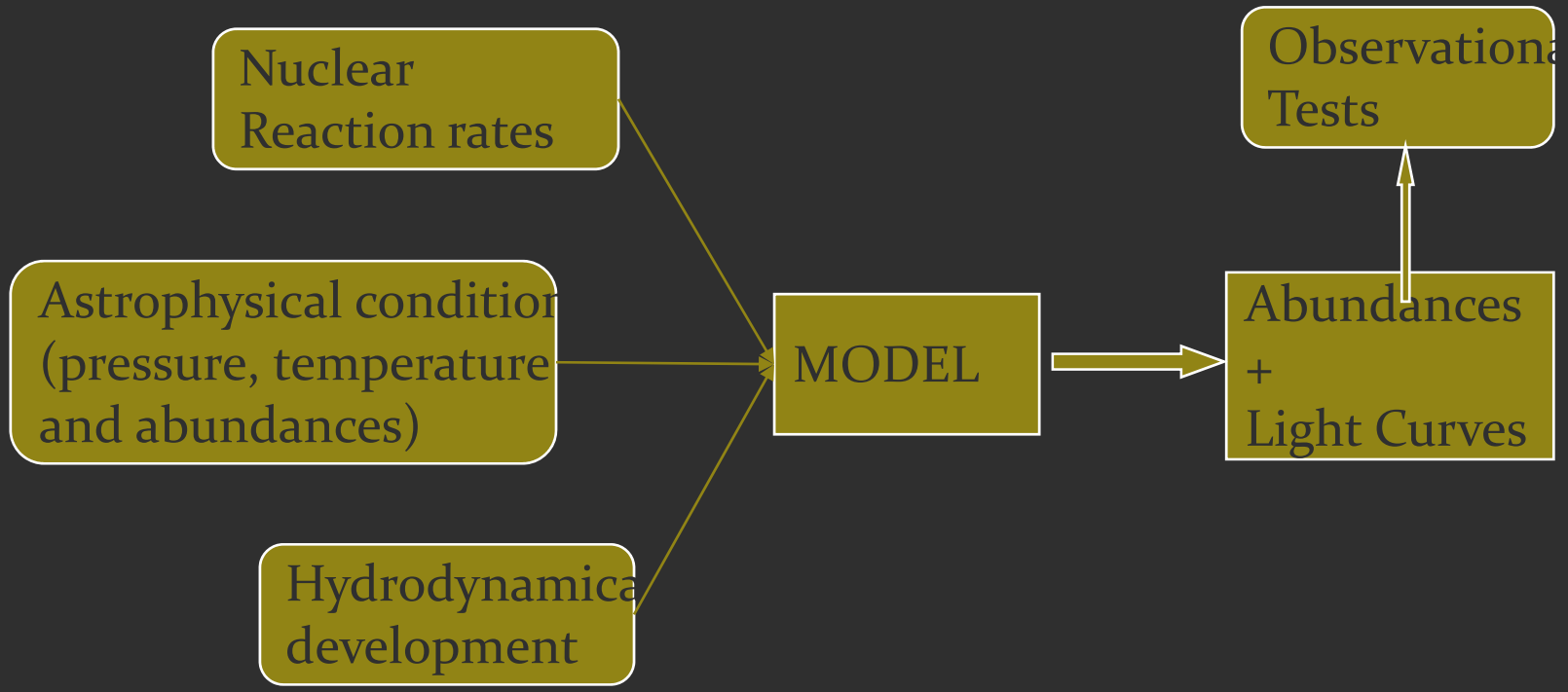

This effort requires an effective collaboration between the different scientific fields

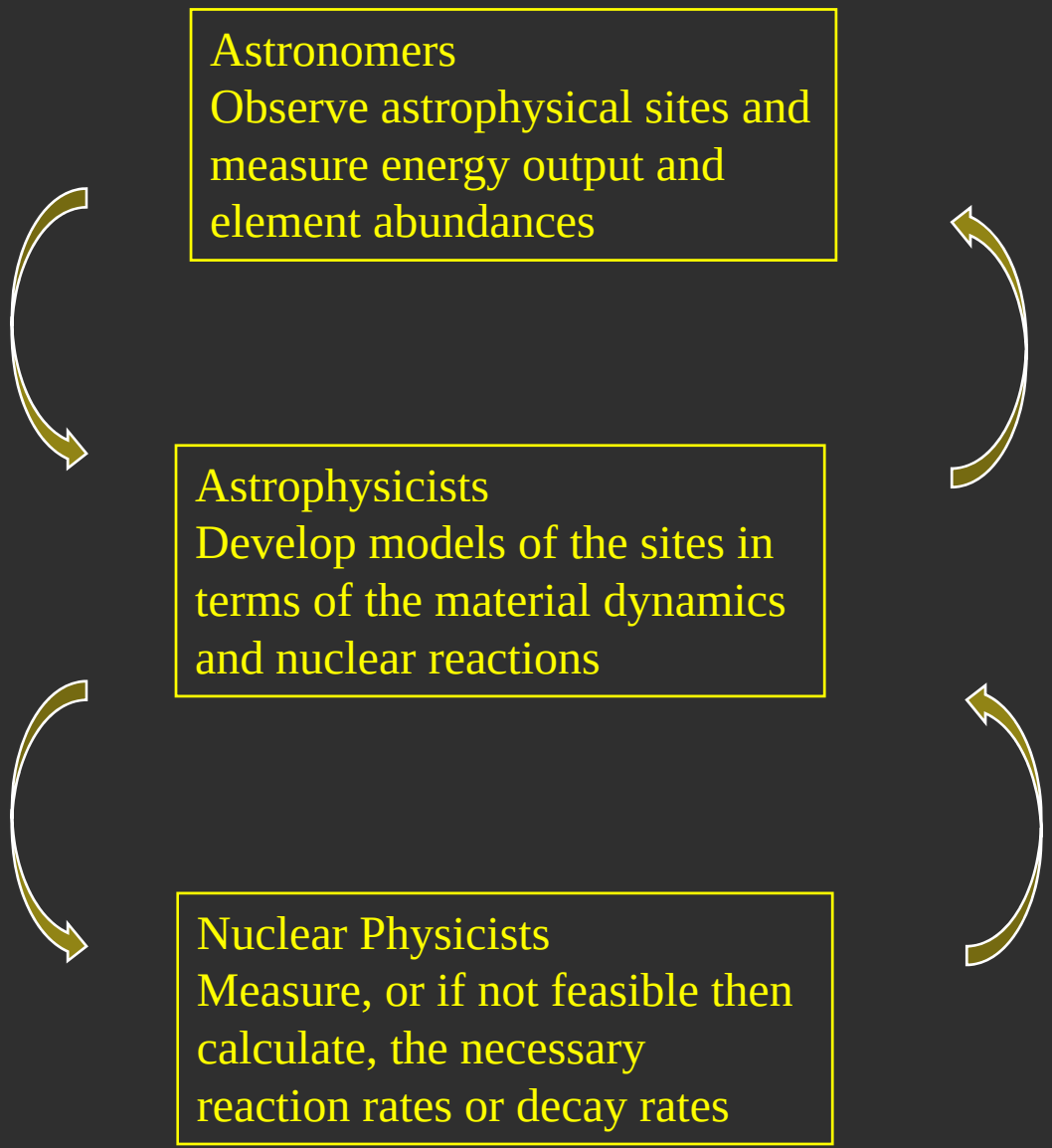

But which reactions are the problem and so need to be measured?

Run sensitivity studies with models to see which reactions have the largest effect on the energy generation or element synthesis. These are the ones for which accurate reaction cross sections are needed.

Novae

ONe nova sensitivity study (Iliadis et al. ApJS (2002)) :

- T-ρ-t profiles from **5 different** hydrodynamic nova simulations
- Network: 1265 nuclear processes, 142 isotopes (H – Ca)
- Variation of **each** of 175 reaction rates within their errors

ONe Nova Models

$^{17}O(p,\gamma)^{18}F$	^{17}O, ^{18}F
$^{17}O(p,\alpha)^{14}N$	^{17}O, ^{18}F
$^{17}F(p,\gamma)^{18}Ne$	^{17}O, ^{18}F
$^{18}F(p,\alpha)^{15}O$	^{16}O, ^{17}O, ^{18}F
$^{21}Na(p,\gamma)^{22}Mg$	^{21}Ne, ^{22}Na, ^{22}Ne
$^{22}Ne(p,\gamma)^{23}Na$	^{22}Ne
$^{23}Na(p,\gamma)^{24}Mg$	^{20}Ne, ^{21}Ne, ^{22}Na, ^{23}Na, ^{24}Mg, ^{25}Mg, ^{26}Mg, ^{26}Al, ^{27}Al
$^{23}Mg(p,\gamma)^{24}Al$	^{20}Ne, ^{21}Ne, ^{22}Na, ^{23}Na, ^{24}Mg
$^{26}Mg(p,\gamma)^{27}Al$	^{26}Mg
$^{26}Al^{g}(p,\gamma)^{27}Si$	^{26}Al
$^{26}Al^{m}(p,\gamma)^{27}Si$	^{26}Mg
$^{29}Si(p,\gamma)^{30}P$	^{29}Si
$^{30}P(p,\gamma)^{31}S$	^{30}Si, ^{32}S, ^{33}S, ^{34}S, ^{35}Cl, ^{37}Cl, ^{36}Ar, ^{37}Ar, ^{38}Ar
$^{33}S(p,\gamma)^{34}Cl$	^{33}S, ^{34}S, ^{35}Cl, ^{36}Ar
$^{33}Cl(p,\gamma)^{34}Ar$	^{33}S
$^{34}S(p,\gamma)^{35}Cl$	^{34}S, ^{35}Cl, ^{36}Ar
$^{34}Cl(p,\gamma)^{35}Ar$	^{34}S
$^{37}Ar(p,\gamma)^{38}K$	^{37}Cl, ^{37}Ar, ^{38}Ar
$^{38}K(p,\gamma)^{39}Ca$	^{38}Ar

X-ray Bursts

Our Type I XRB sensitivity study: rate variations

Important reaction rates to determine!

Reaction	AME03 Q-value	Reaction	AME03 Q-value
$^{22}Mg(\alpha,p)^{25}Al$	3655(1)	$^{71}Br(p,\gamma)^{72}Kr$	4167(568)
$^{25}Si(\alpha,p)^{28}P$	6119(11)	$^{75}Rb(p,\gamma)^{76}Sr$	4311 (38)
$^{26g}Al(\alpha,p)^{29}Si$	4820.68(6)	$^{82}Zr(p,\gamma)^{83}Nb$	2055(387)[b]
$^{29}S(\alpha,p)^{32}Cl$	5306(50)	$^{84}Nb(p,\gamma)^{85}Mo$	4513(409)[b]
$^{30}S(\alpha,p)^{33}Cl$	2077(3)	$^{84}Zr(p,\gamma)^{85}Nb$	2946(297)[b]
$^{30}P(\alpha,p)^{33}S$	1521.36(34)	$^{85}Mo(p,\gamma)^{86}Tc$	1393(409)[b]
$^{31}Cl(p,\gamma)^{32}Ar$	2422(50)	$^{86}Mo(p,\gamma)^{87}Tc$	1855(530)[b]
$^{32}S(\alpha,\gamma)^{36}Ar$	6640.76(14)	$^{87}Mo(p,\gamma)^{88}Tc$	2304(300)[b]
$^{56}Ni(\alpha,p)^{59}Cu$	−2411(11)	$^{92}Ru(p,\gamma)^{93}Rh$	2054(499)[b]
$^{57}Cu(p,\gamma)^{58}Zn$	2277(52)	$^{93}Rh(p,\gamma)^{94}Pd$	4467(566)[b]
$^{59}Cu(p,\gamma)^{60}Zn$	5120(11)	$^{96}Ag(p,\gamma)^{97}Cd$	3321(566)[b]
$^{61}Ga(p,\gamma)^{62}Ge$	2442(149)[b]	$^{102}In(p,\gamma)^{103}Sn$	3554(318)[b]
$^{65}As(p,\gamma)^{66}Se$	2030(424)[b]	$^{103}In(p,\gamma)^{104}Sn$	4281(107)
$^{69}Br(p,\gamma)^{70}Kr$	2489(399)[b]	$^{103}Sn(\alpha,p)^{106}Sb$	5508(432)[b]

b: Q and ΔQ estimated from systematics

No experimental rate information available for any of these!

Parikh, José, Moreno and Iliadis, ApJS 178 (2008) 110.

3. A Technique to measu
$^{12}C(\alpha,\gamma)^{16}O$

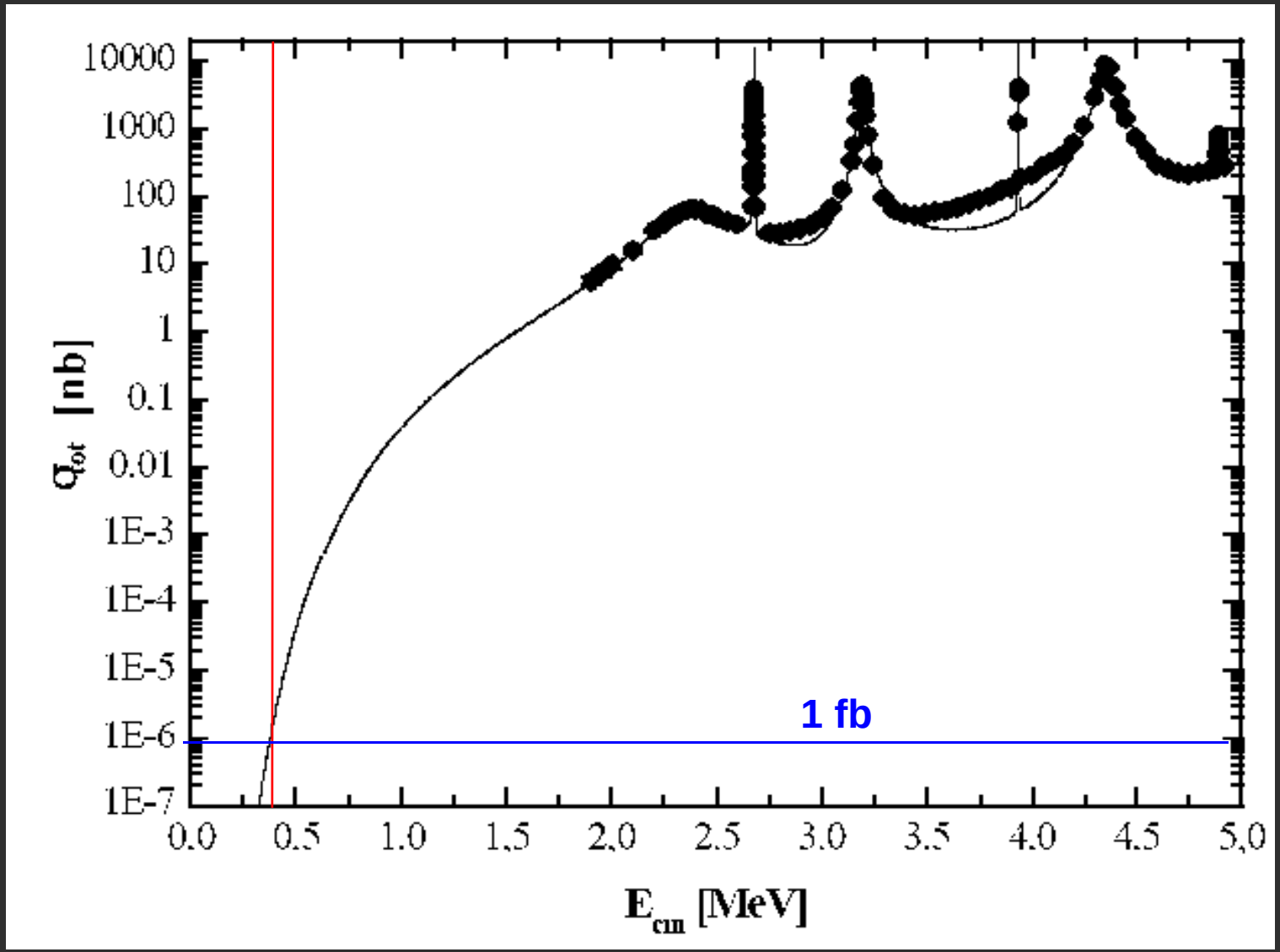
10000
1000
100
10
1
0.1
0.01
1E-3
1E-4
1E-5
1E-6
1E-7
σ_{tot} [nb]
1 fb
0.0
0.5
1.0
1.5
2.0
2.5
3.0
3.5
4.0
4.5
5.0
E_{cm} [MeV]

$^{12}C(\alpha,\gamma)^{16}O$

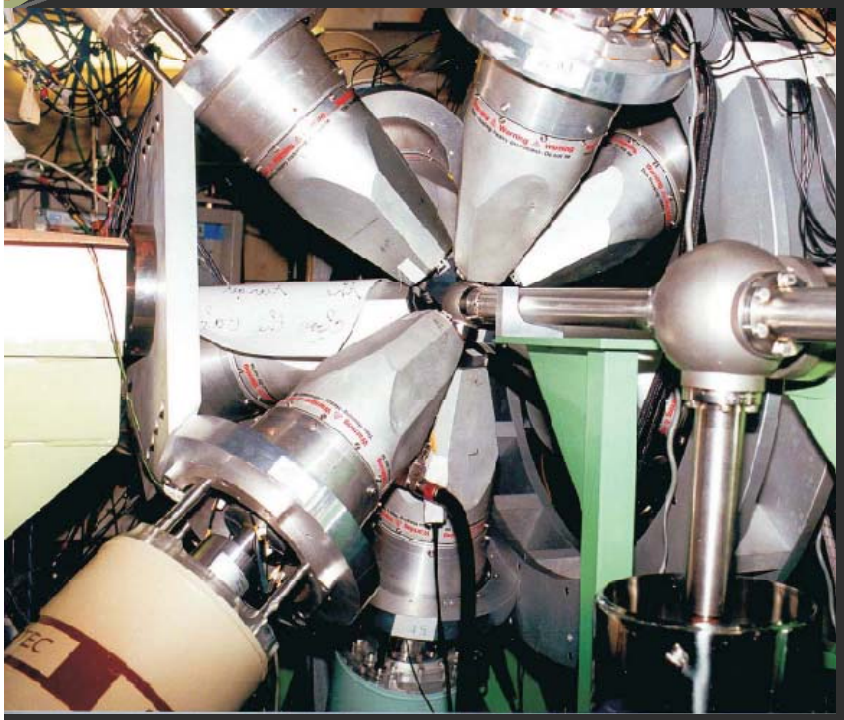

R. Kunz, thesis, 2002

- 'High' intensity α-beams
- 'thin' targets
- 'Low' detection efficiency

Luminosity= I t ε ~ 10^{31}/(sec cm^2)

(1 count/day/1 pb)

Step 1: Measure the time-inverse reaction: $^{16}O(\gamma,\alpha)^{12}C$

Advantage:

- **Larger cross section for time-inversed reaction**

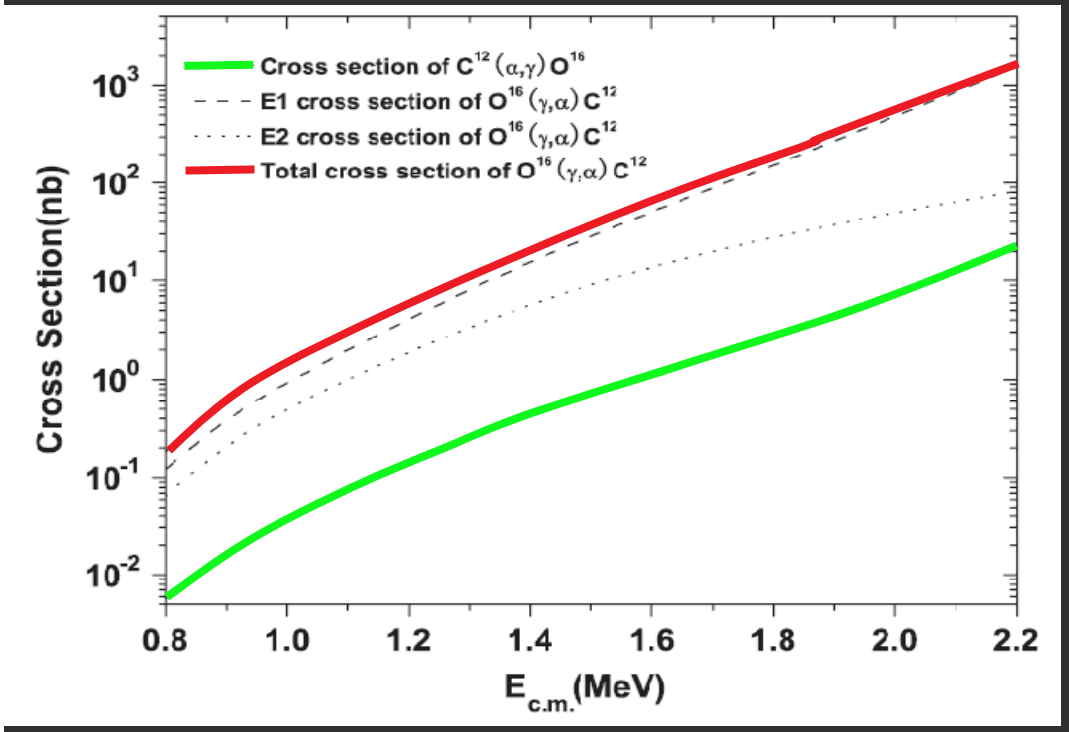

Factor of 10^2 improvement

Disadvantage:

- **Lower beam intensities at the HIγS facility (10^{-6})**

Step 2: Use a liquid target for the (γ,α) measurement (x 10^6)

Advantages:

- The γ's (8-10 MeV) have a much larger range than charged particles (α or ^{12}C)
- use thicker targets (~10 g/cm^2 (e.g. water) vs. 10 μg/cm^2) (10^6)

Disadvantages:

- Need a detector that is insensitive to γ's but sensitive to charged particles (e.g. α's)

1. Accelerator: HIγS

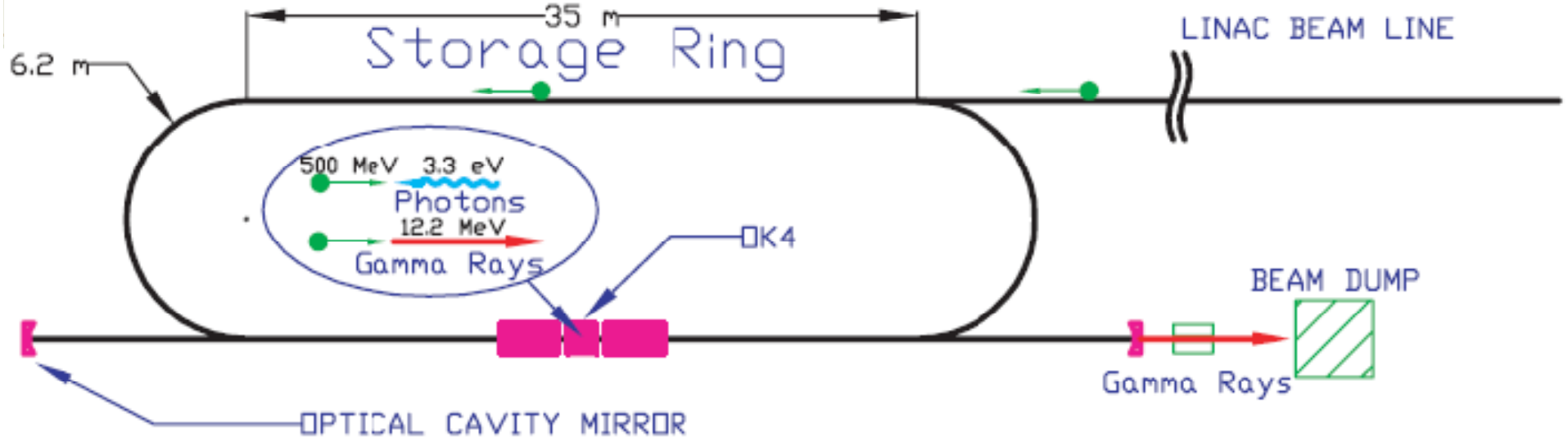

Relativistic electron (E_e)

I_γ ~ $10^{7\text{-}8}$ photons/sec

Laser light (λ_L)

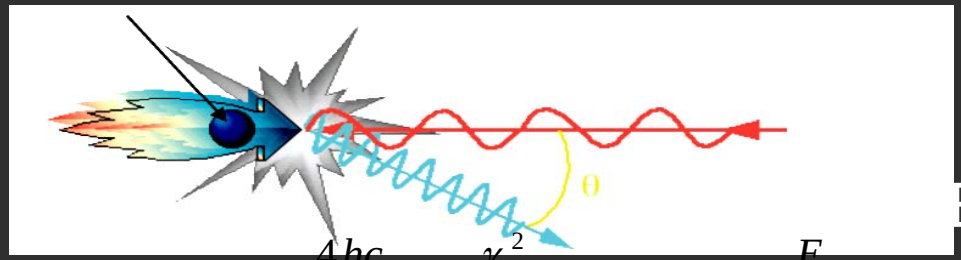

$$E_\gamma = \frac{4hc}{\lambda_L}\cdot\frac{\gamma^2}{1+\gamma^2\theta^2}, \quad \gamma = \frac{E_e}{m_e c^2}$$

ex. λ_L=1.064μm, E_e=800MeV

⇒ E_γ = 11MeV

$E_\gamma(\theta)$

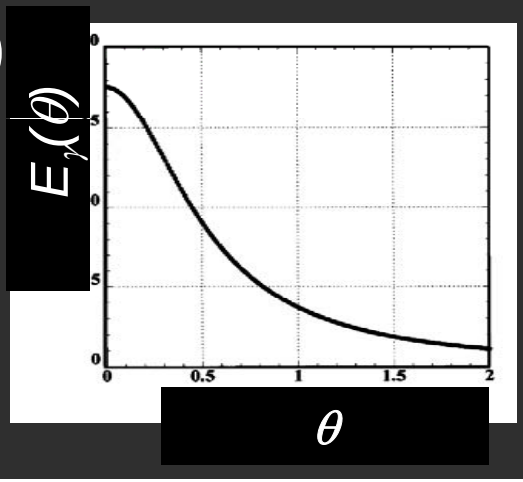

Proof of Principle of a superheated bubble chamber for the $^{19}F(\gamma,\alpha)^{15}N$ reaction

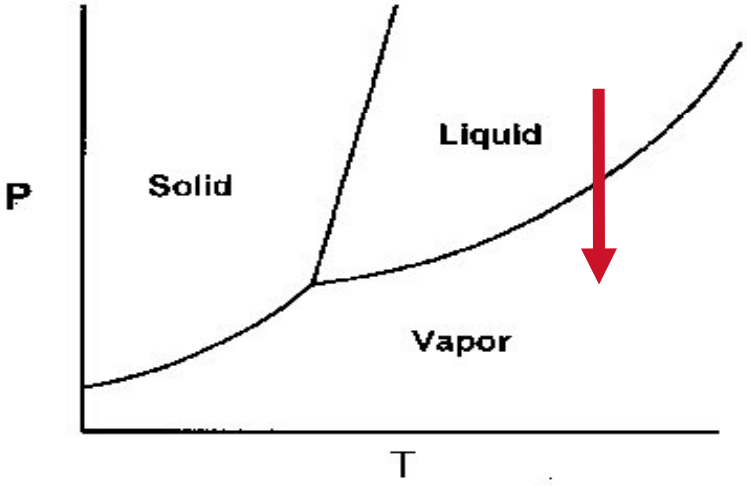

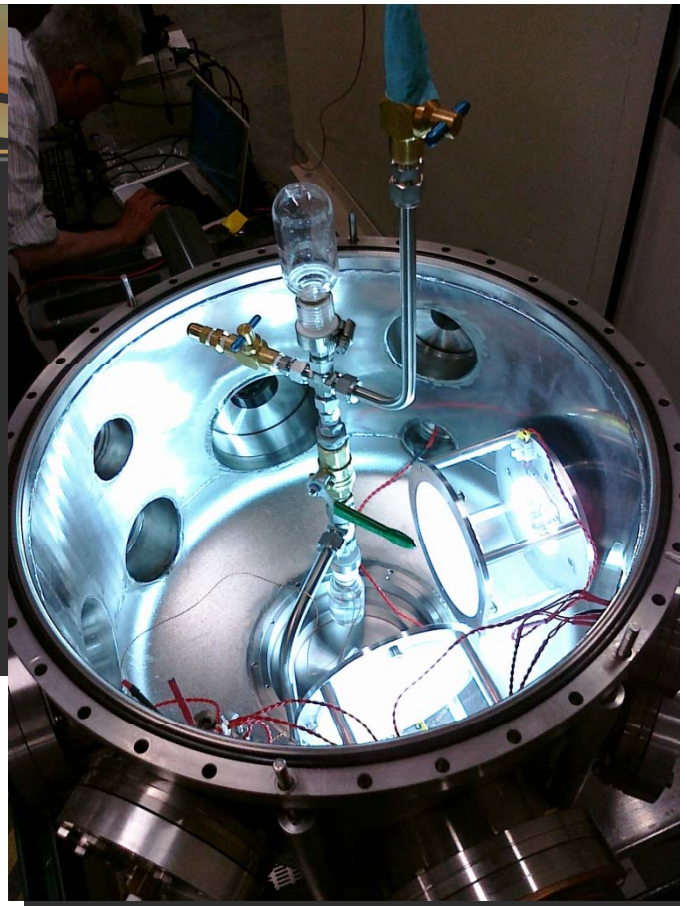

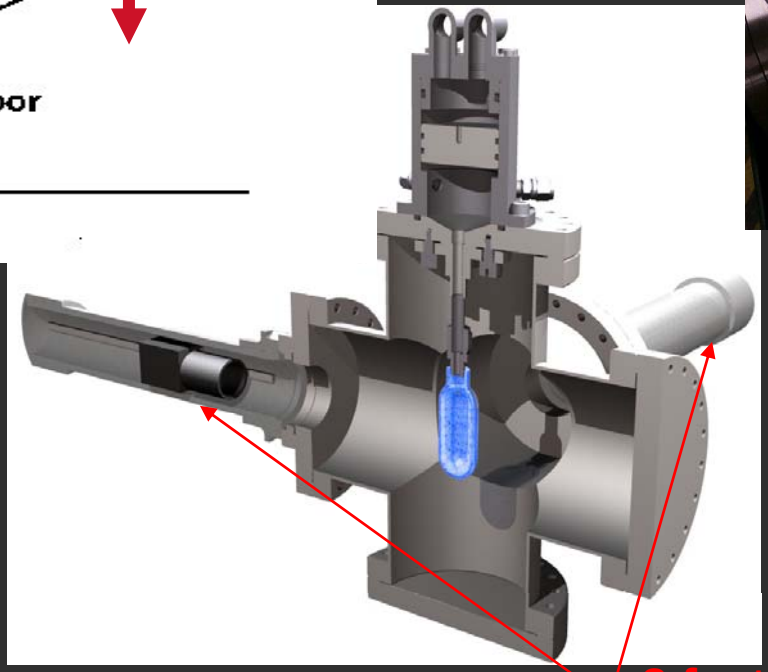

2 fast cameras

P~ 1-6 atm
T~20-50 C

A ‘successful’ bubble

Dead time ~1-2 sec → detector for low count rates

Conditions for $^{19}F(\gamma,\alpha)^{15}N$ in C_4F_{10}
E_γ=5-6 MeV

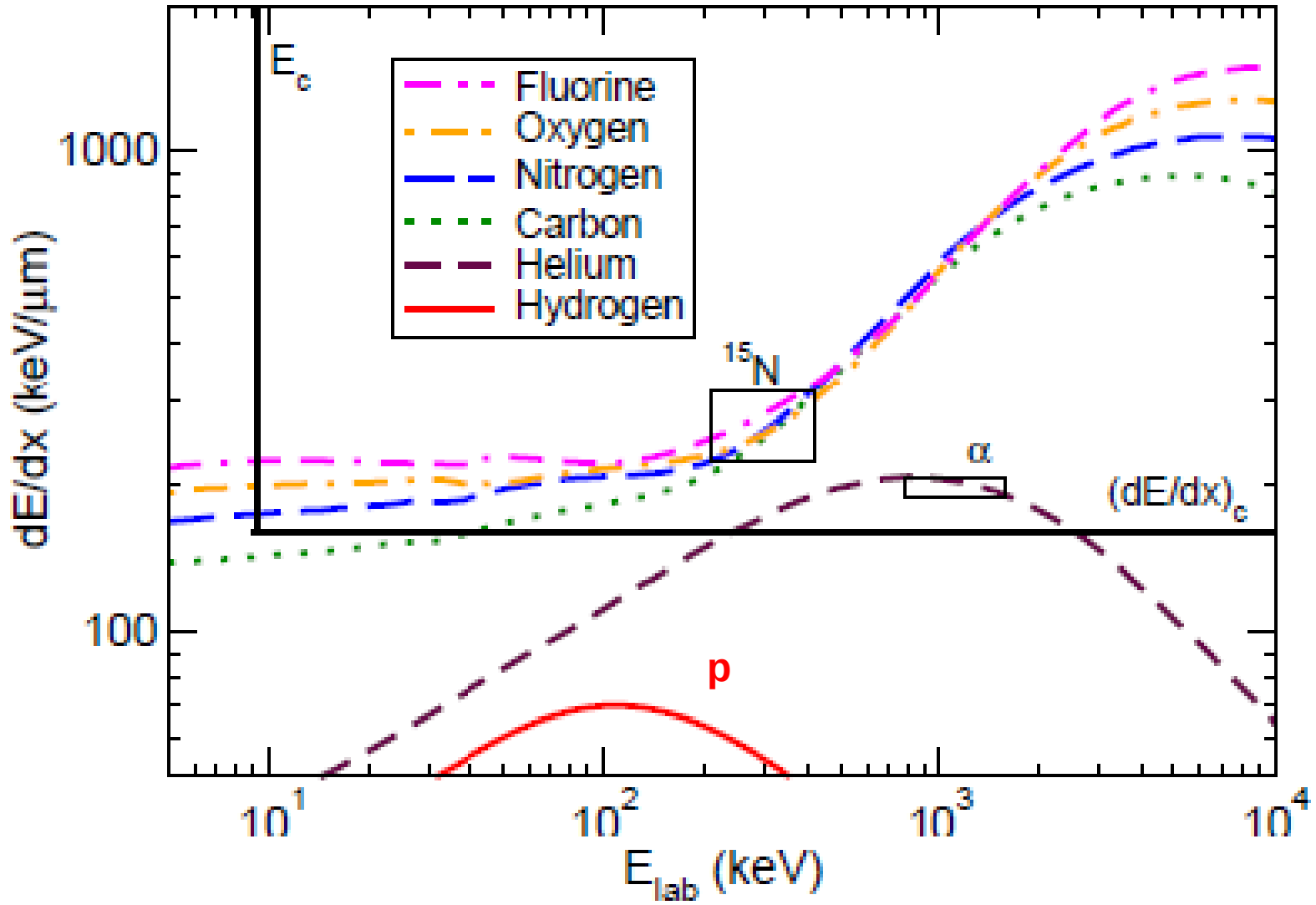

Position sensitivity in 3D

Cu
collimator

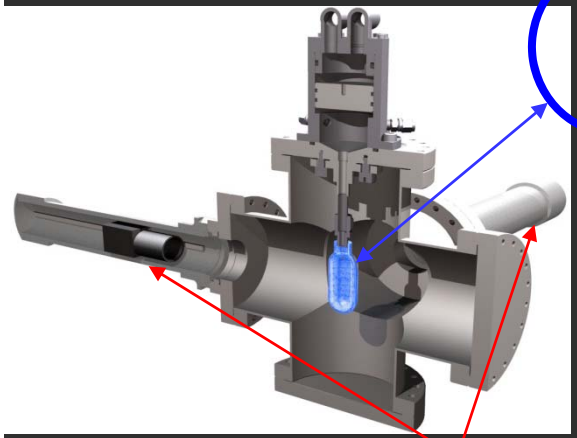

2 fast cameras

Camera-2'

Camera-1'

$\Delta x < 1$ mm

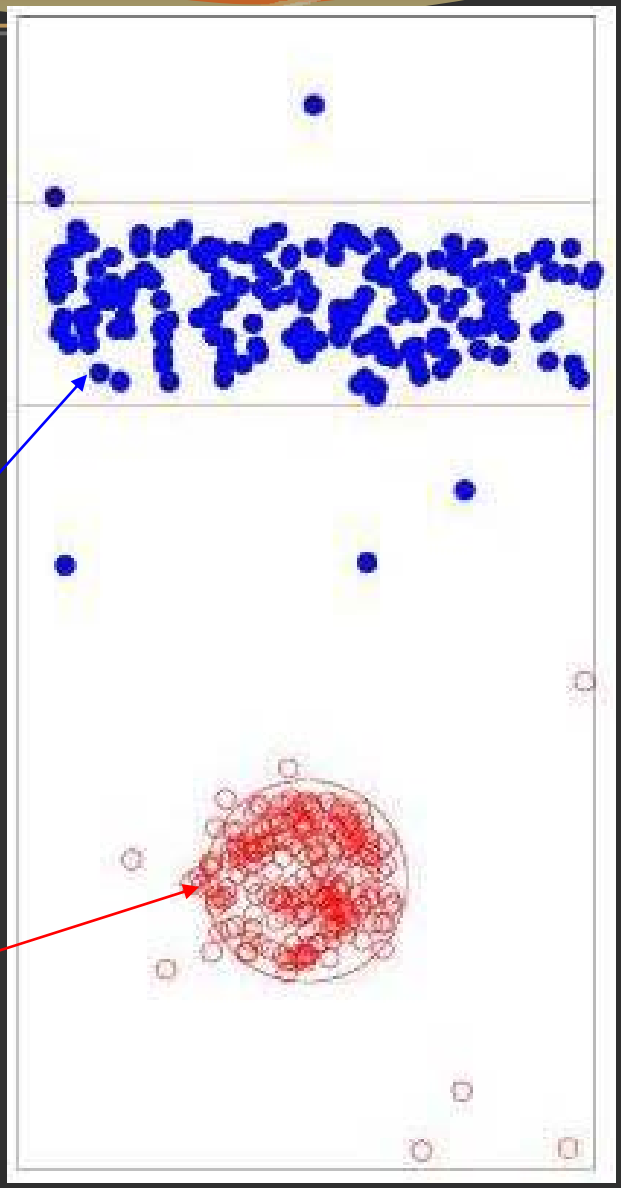

In a classical picture the excess neutrons form a skin around the proton/neutron core with *N Z. An oscillation of the skin vs the core would lead* to an electric dipole excitation mode. Because this mode bears resemblance to a “mini” giant dipole resonance it is often called pygmy dipole resonance (PDR).
perform very sensitive Ca(γ , γ`) experiments up to an excitation energy of 10.5 MeV
performed photon scattering experiments on ^{40}Ca and ^{48}Ca

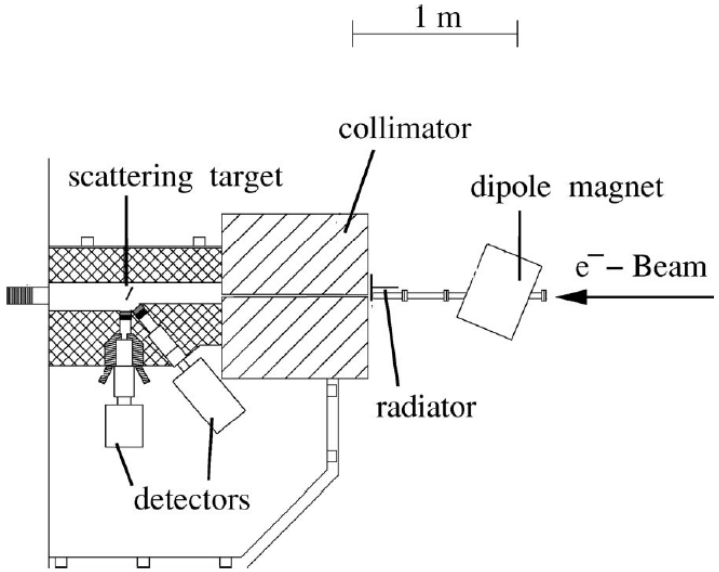

FIG. 1. The NRF setup at the S-DALINAC at Darmstadt University of Technology. The monoenergetic electron beam with energies up to 10 MeV and currents of typically 35 μA is stopped in a Cu radiator. The resulting γ radiation with a continuous energy distribution is collimated by a 95.5 cm long Cu collimator and strikes the scattering target. The decays of the excited nuclei to the ground state or other excited levels are detected by two HPGe detectors located at angles of 90° and 130° relative to the incoming photon beam.

VOLUME 85, NUMBER 2 PHYSICAL REVIEW LETTERS 10 JULY 2000

Measurement of the Dipole and Electric Quadrupole Strength Distributions up to 10 MeV in the Doubly Magic Nuclei ^{40}Ca and ^{48}Ca

T. Hartmann, J. Enders, P. Mohr, K. Vogt, S. Volz, and A. Zilges
Institut für Kernphysik, Technische Universität Darmstadt, Schlossgartenstrasse 9, D-64289 Darmstadt, Germany
(Received 23 February 2000)

The doubly magic nuclei ^{40}Ca and ^{48}Ca have been studied in high resolution photon scattering experiments. We have derived absolute dipole and quadrupole excitation strengths up to 10 MeV. Evidence was found for a two-phonon quadrupole-octupole state in ^{48}Ca. At higher energies in contrast to ^{40}Ca, a concentration of dipole strength is observed in ^{48}Ca which is discussed in terms of a pygmy resonance originating from the large neutron excess.

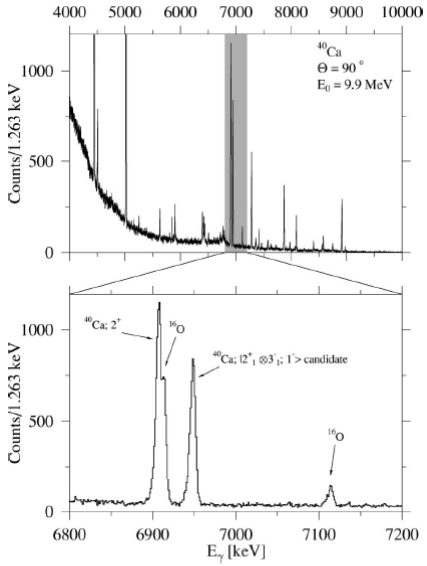

FIG. 7. Photon spectrum of ^{40}Ca (γ,γ') with an endpoint energy of 9.9 MeV measured at 90° with respect to the incoming beam. The levels at 5020 and 4444 keV exceeding the scale are transitions in ^{11}B. The lower part shows an enlarged view of the energy region between 6.8 and 7.2 MeV to demonstrate the energy resolution and the excellent peak-to-background ratio. Shown are singles spectra. No background was subtracted.

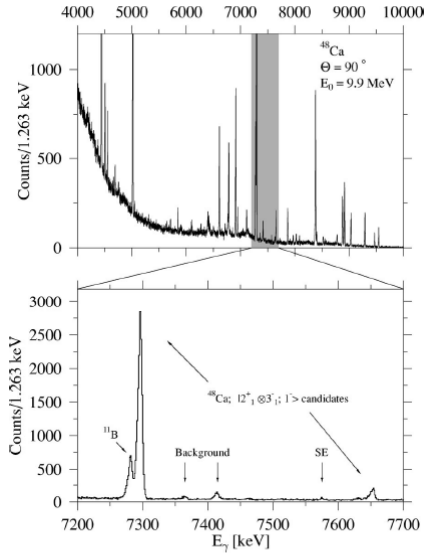

FIG. 8. Photon spectrum of ^{48}Ca (γ,γ') with an endpoint energy of 9.9 MeV taken at 90° with respect to the incoming beam. The peaks at 5020, 4444, and 7282 keV exceeding the scale are transitions in ^{11}B. The lower part shows an enlarged view of the energy region between 7.1 and 7.4 MeV to demonstrate the energy resolution and the excellent peak-to-background ratio.

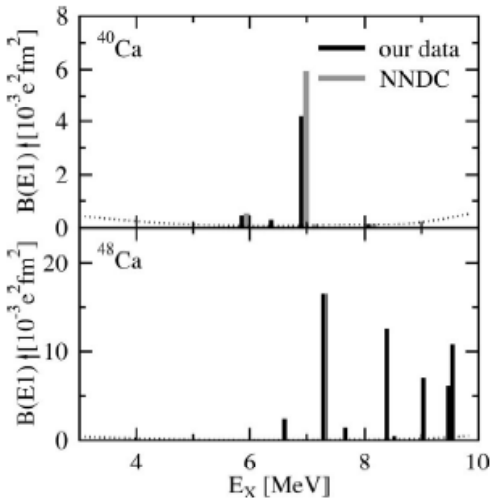

FIG. 9. Electric dipole strength distributions for ^{40}Ca (upper part) and ^{48}Ca (lower part). The strengths of ^{40}Ca are compared to NNDC data [44] which are mainly based on the results of Moreh *et al.* [53]. Please note the different scales. The dotted line shows the sensitivity limit of the measurements.

2. Comparison with previous experiments

Another experimental comparison of the electric dipole strength distributions of the two calcium isotopes was performed recently [56]. Here, ^{40}Ca and ^{48}Ca were studied in ^{40,48}Ca(^{86}Kr,^{86}Kr′)^{40,48}Ca heavy ion scattering reactions. The results for the summed $E1$ strength below 10 MeV from this study is 7.5(18)% and 6.7(33)% for the EWSR in ^{40}Ca and ^{48}Ca, respectively. This is in sharp contrast to our results.

Heavy-ion scattering, however, does not allow the electromagnetic transition strength to be determined model independently. Our experiments are model independent, exhibit high resolution resolving single excitations and are characterized by a low detection limit. Therefore our results exclude those from Ref. [56] clearly.

- Thank you for your attention